Supplementary Figures

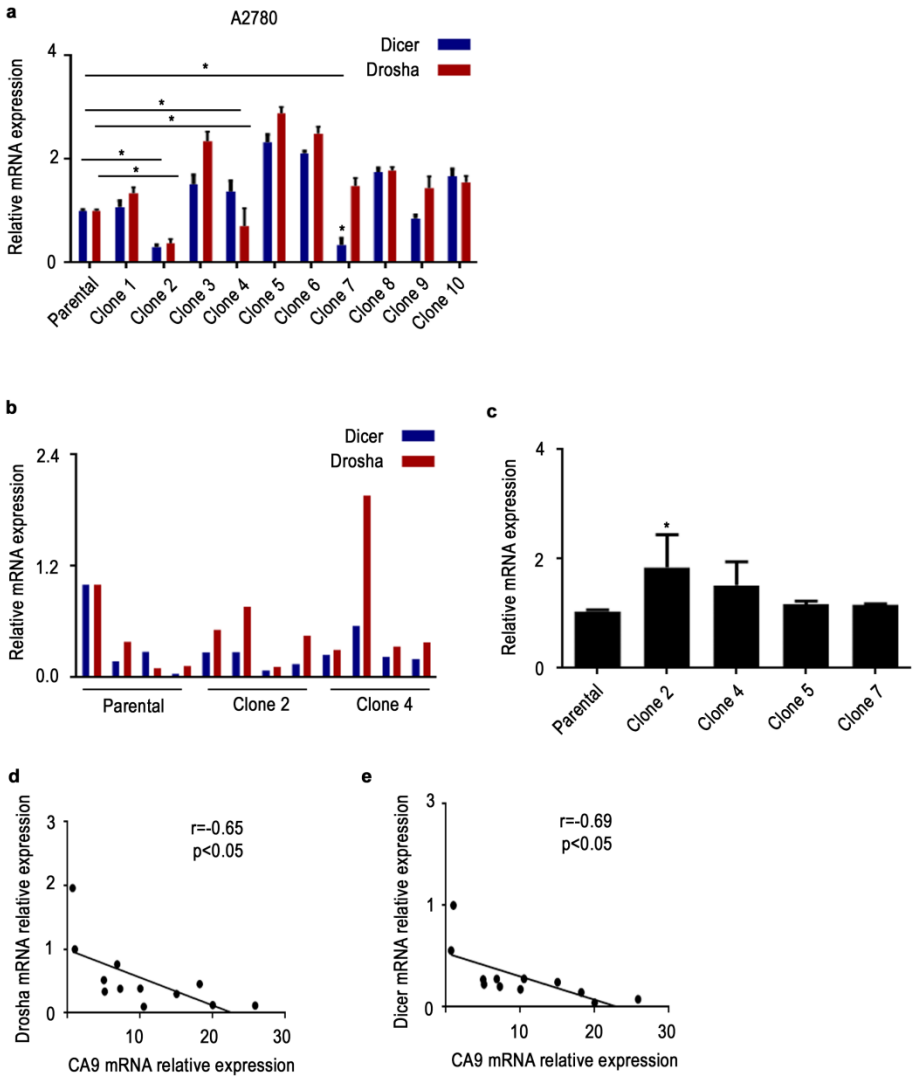

Supplementary Figure 1: (**a**) mRNA expression levels of Drosha and Dicer in single-cell clones derived from A2780 cells. (**b**) mRNA expression levels of Drosha and Dicer in individual tumor samples from mice injected with A2780 clones (n = 4 per group). (**c**) Expression of CA9 (hypoxia marker) in single cells clones of A2780 cell line, compared to parental cells. (**d-e**) Spearman correlation between mRNA expression levels of Dicer and Drosha with carbonic anhydrase 9 (CA9) levels in individual tumor samples from mice injected with parental cells and single-cell clones. Data are presented as mean ± standard error of the mean of n ≥ 3 independent experimental groups. *p < 0.05 (Student t test).

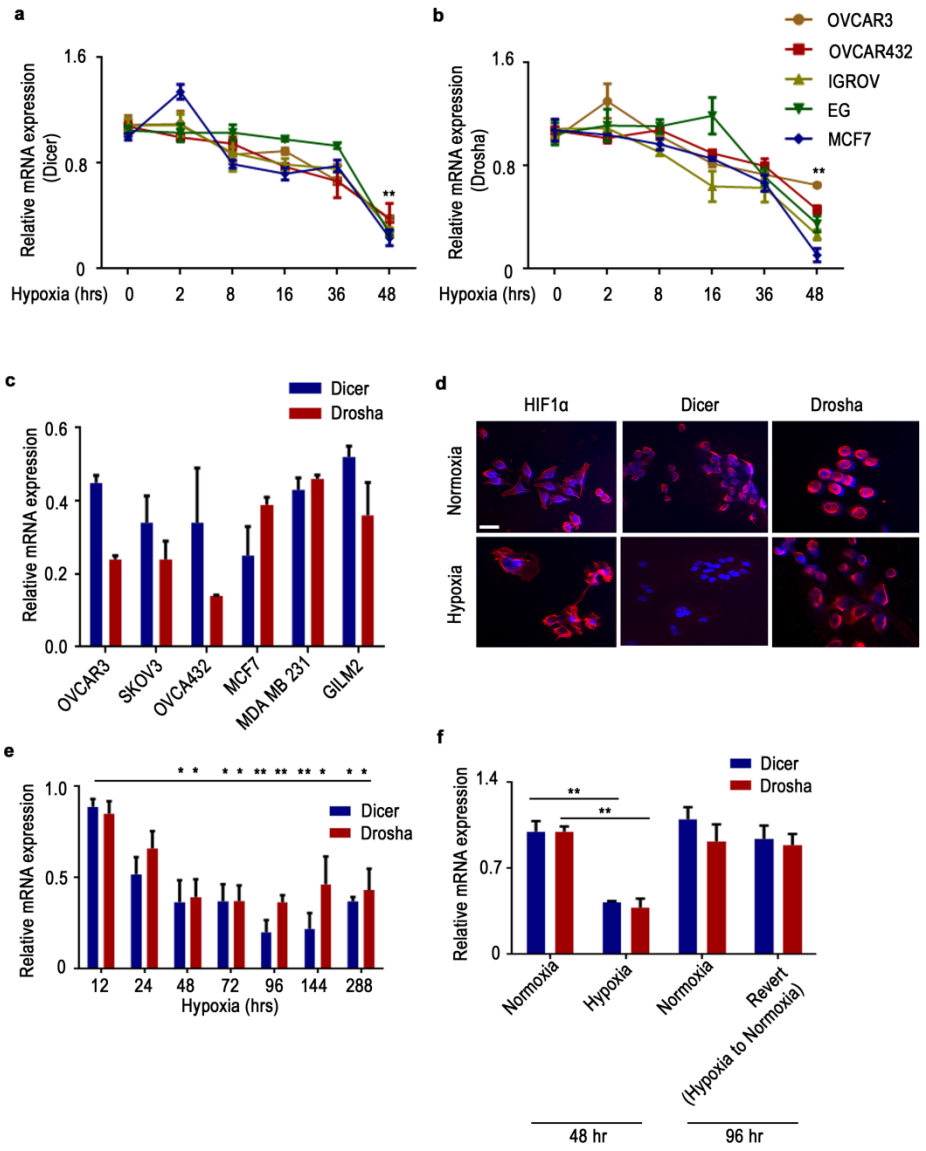

Supplementary Figure 2: (**a** and **b**) Drosha and Dicer mRNA expression levels under hypoxic conditions for several ovarian and breast cancer cell lines at different time points. (**c**) Drosha and Dicer mRNA expression levels in several ovarian and breast cancer cell lines 48 hrs following hypoxia treatment. Data are normalized to normoxic conditions. (**d**) Protein levels of HIF1α, Dicer, and Drosha in OVCAR3 cells under hypoxic and normoxic conditions at 48 hr time point. Scale bar: 200 µm. (**e**) mRNA expression levels of Drosha and Dicer in A2780 cells after long durations of hypoxic conditions. Data are normalized to normoxic conditions. (**f**) mRNA expression levels of Drosha and Dicer in A2780 cells after 48 hr of hypoxia treatment and reversal to normoxic condition. Data are presented as mean ± standard error of the mean of n ≥ 3 independent experimental groups. *p < 0.05, **p < 0.01 (Student *t* test).

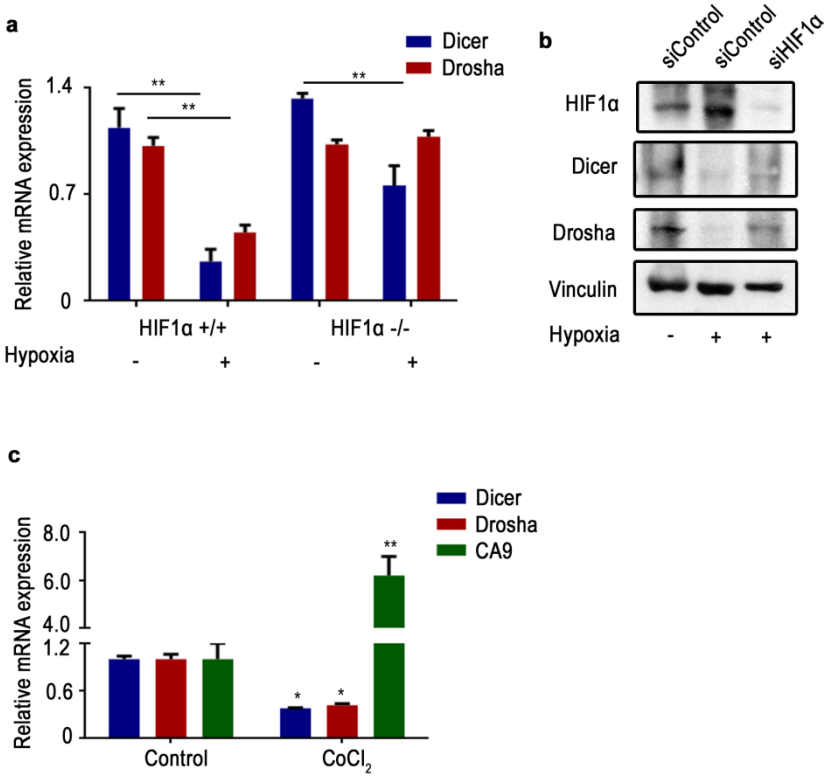

Supplementary Figure 3: (**a**) Drosha and Dicer levels in mouse embryonic fibroblasts with wild-type HIF1α (+/+) or HIF1α-knockout (-/-) mouse embryonic fibroblasts under normoxic and hypoxic conditions for 48 hrs. (**b**) Western blot analysis of the protein expression of HIF1α, Drosha, and Dicer in cells treated with siControl or siHIF1α in normoxic or hypoxic conditions (48 hr). Vinclulin used as loading control. (**c**) Drosha, Dicer, and CA9 levels in $CoCl_2$ treated A2780 cells under normoxia. Data are presented as mean ± standard error of the mean of n ≥ 3 independent experimental groups. *p < 0.05, **p < 0.01 (Student *t* test).

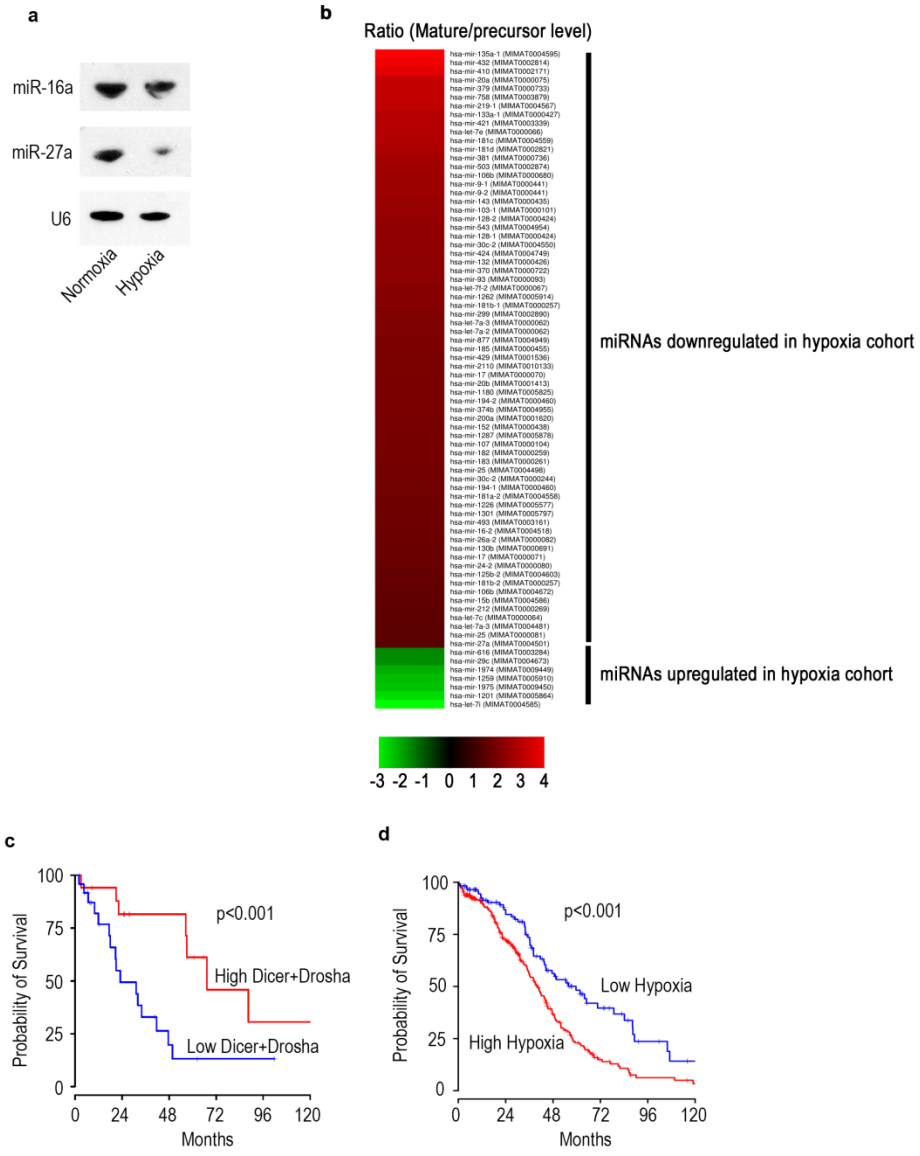

Supplementary Figure 4: (a) Northern blot data showing expression of mature miRNAs in RNA samples from normoxia and hypoxia exposed A2780 cells. Probing for U6 used as loading control. **(b**) Heat map depicting the ratio of mature miRNAs to precursor miRNAs in cells with high or low Drosha and Dicer expression levels. **(c**) Kaplan-Meier overall survival curves for Cancer Genome Atlas project (TCGA) samples analyzed for low and high Drosha and Dicer expression levels ($p < 0.001$). (**d**) Analysis of TCGA samples for hypoxia levels and correlation with overall survival duration, plotted using the Kaplan-Meier method ($p < 0.001$).

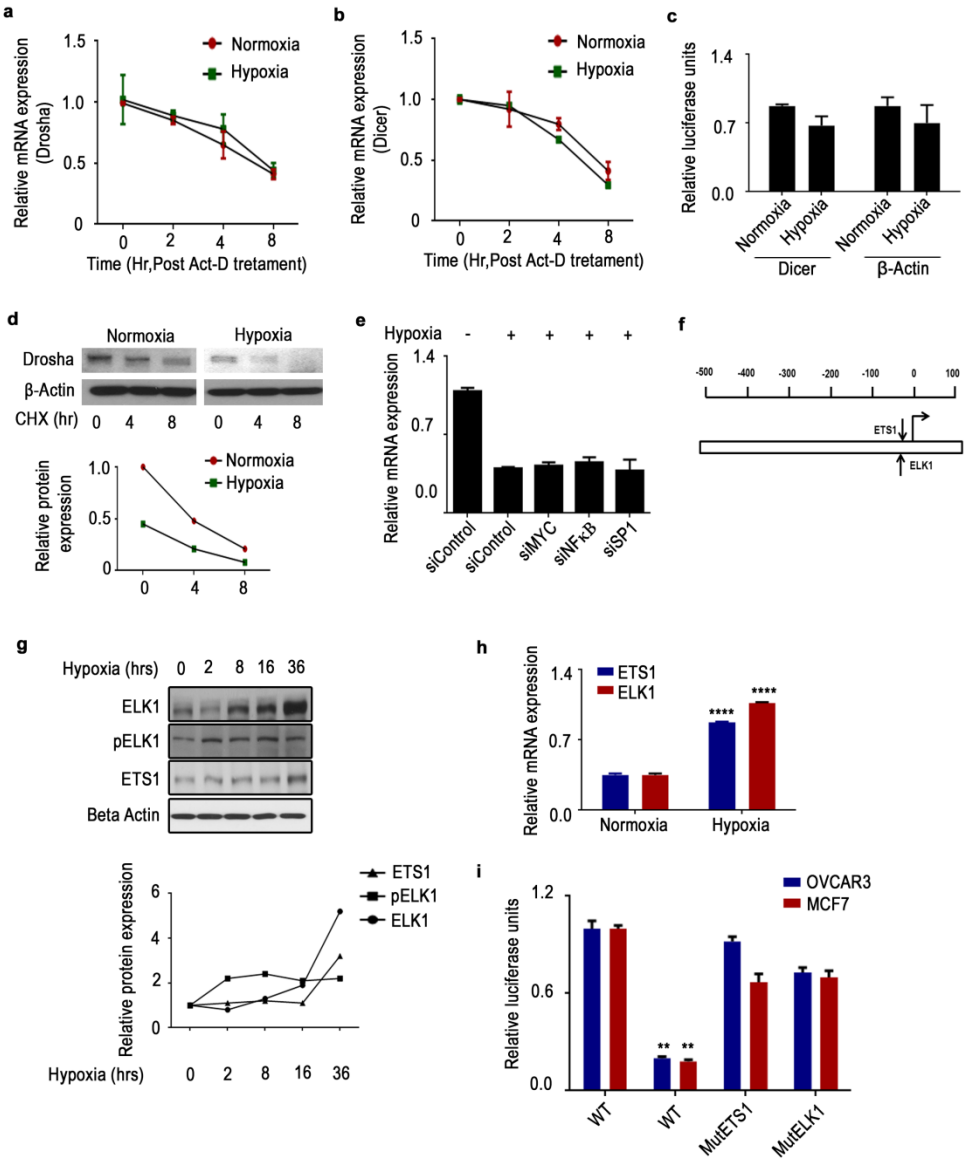

Supplementary Figure 5: (**a-b**) Drosha and Dicer mRNA half-life in A2780 cells exposed to normoxia and hypoxia. (**c**) Luciferase reporter activity of Dicer promoter region under hypoxia exposure compared to normoxia in A2780 cells. (**d**) Stability of Drosha protein in A2780 cells exposed to normoxia and hypoxia. Cycloheximide at 100ug/ml was used to block protein synthesis. (**e**) Drosha mRNA expression after siRNA mediated silencing of Myc, NF-kB, and SP-1 transcription factors under hypoxia exposure in A2780 cells. (**f**) Graphical representation of ETS1 and ELK1 binding sites on the Drosha promoter region. (**g**) ETS, ELK1, and pELK1 expression in A2780 cells across several time points. Quantitative data from Western blot are shown. (**h**) ETS1 and ELK1 mRNA expression levels under hypoxic conditions compared to normoxic conditions in MCF7 cells. (**i**) Luciferase reporter activity for the wild-type (WT)

Drosha promoter region and the ETS1 or ELK1 binding site–mutant Drosha promoter region under hypoxic conditions in OVCAR3 and MCF7 cells. Data are presented as mean ± standard error of the mean of n ≥ 3 independent experimental groups. **p<0.01, ****p < 0.0001 (Student *t* test).

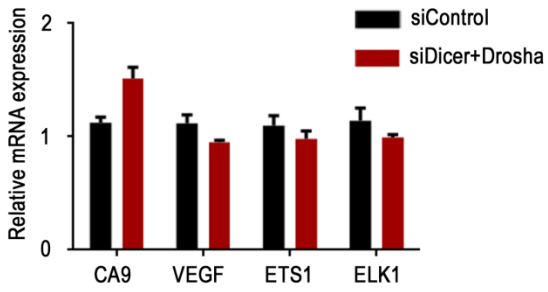

Supplementary Figure 6: Expression of CA9, VEGF, ETS1, and ELK1 in A2780 cells treated with siRNA against Dicer and Drosha. Data are presented as mean ± standard error of the mean of n ≥ 3 independent experimental groups.

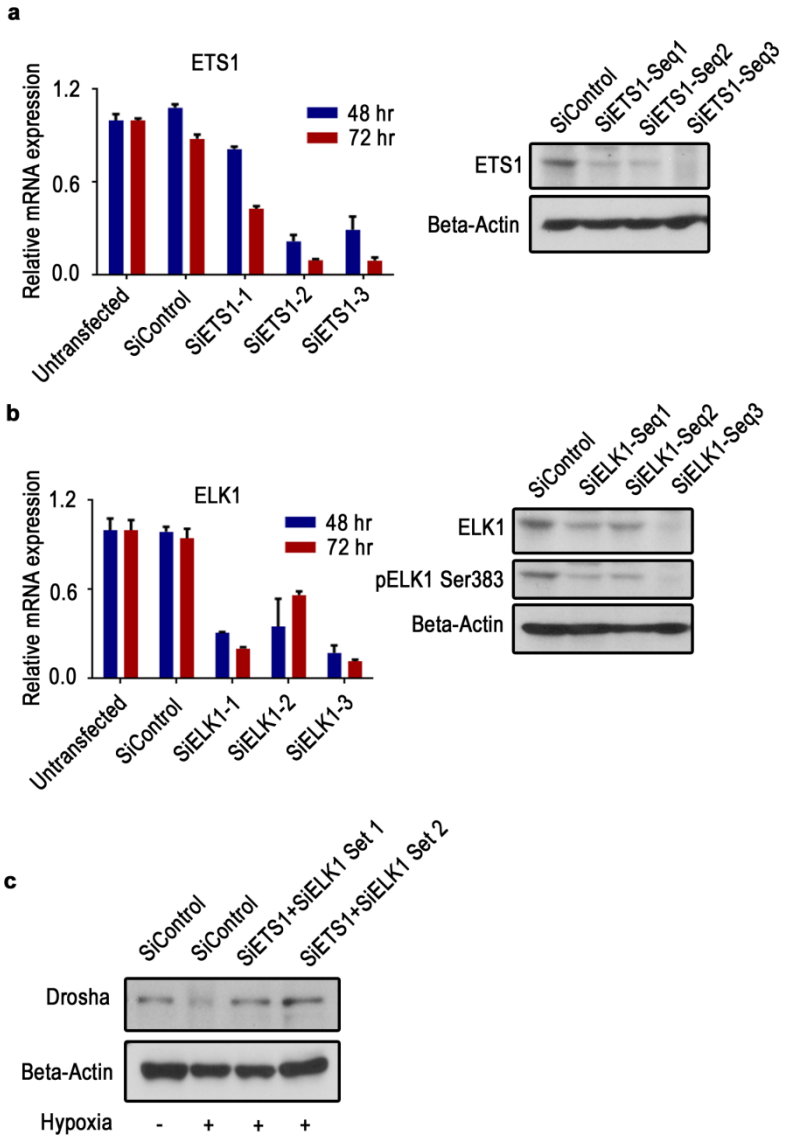

Supplementary Figure 7: MRNA and protein expression levels of ETS1 (**a**) and ELK1 (**b**) after siRNA-mediated silencing of respective genes using 3 different sequences of siRNA in A2780 cells. (**c**) Western blot showing Drosha expression under hypoxic conditions, after ETS1 and ELK1 gene knockdown with 2 independent siRNA sequences in A2780 cells. Data are presented as mean ± standard error of the mean of n ≥ 3 independent experimental groups.

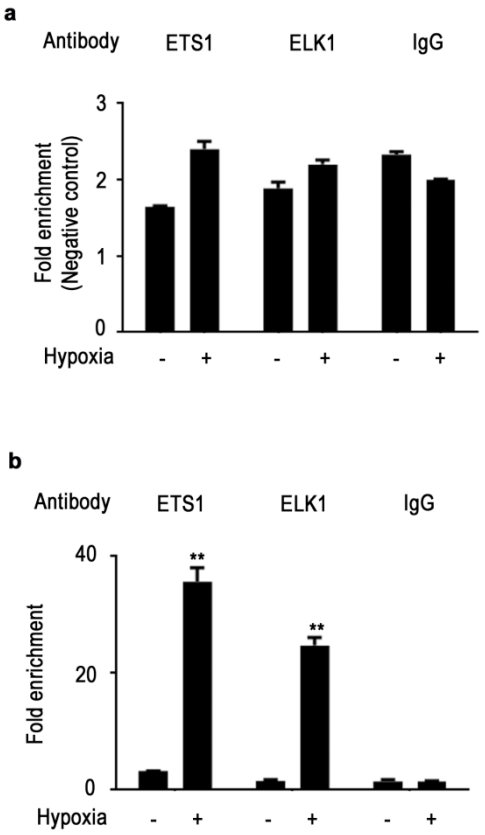

Supplementary Figure 8: (**a**) Fold enrichment 1000 base pair upstream of ETS1 and ELK1 binding region at the Drosha promoter under hypoxia conditions in A2780 cells. (**b**) Fold enrichment of ETS1 and ELK1 binding at the Drosha promoter region under hypoxic conditions (MCF7), assessed using chromatin immunoprecipitation assays. Data are presented as mean ± standard error of the mean of n ≥ 3 independent experimental groups. **p<0.01 (Student *t* test).

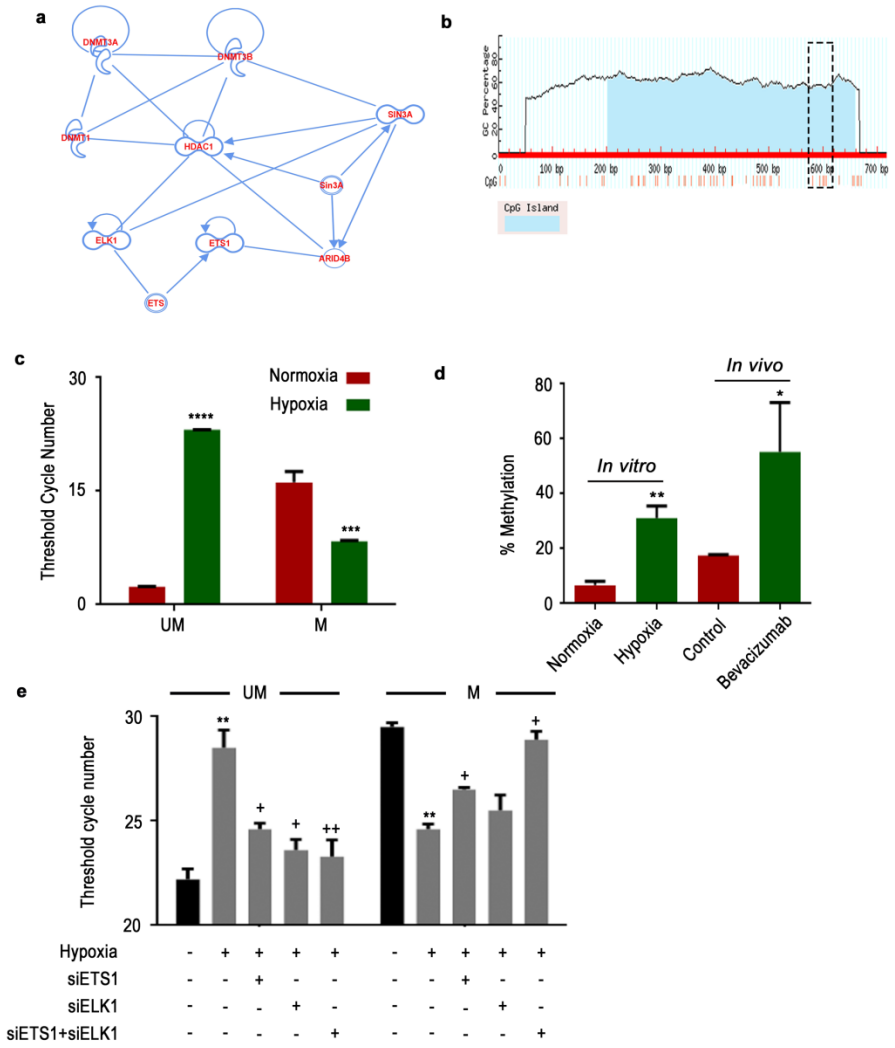

Supplementary Figure 9: (a and **b**) Ingenuity pathway network analysis of possible interacting molecules of ETS1 and ELK1 and graphical representation of the CpG island in the Drosha promoter region. Dotted box highlights the area covered by methylation-specific primers. (**c**) Threshold cycle number of unmethylated (UM) and methylated (M) targeting primers under normoxic and hypoxic conditions in MCF7 cells. (**d**) Percentage methylation in Drosha promoter region CpG island measured using methylation specific restriction enzyme analysis. DNA from A2780 cells exposed normoxia and hypoxia were used. (**e**) Threshold cycle number of unmethylated (UM) and methylated (M) targeting primers under normoxic and hypoxic conditions in A2780 cells treated with hypoxia and siETS1, siELK1 or combinations. Data are presented as mean ± standard error of the mean of n ≥ 3 independent experimental groups. *p<0.05, **p<0.01, ***p<0.001 compared to normoxia control, +p<0.05, ++p<0.01, compared to hypoxia control. (Student *t* test).

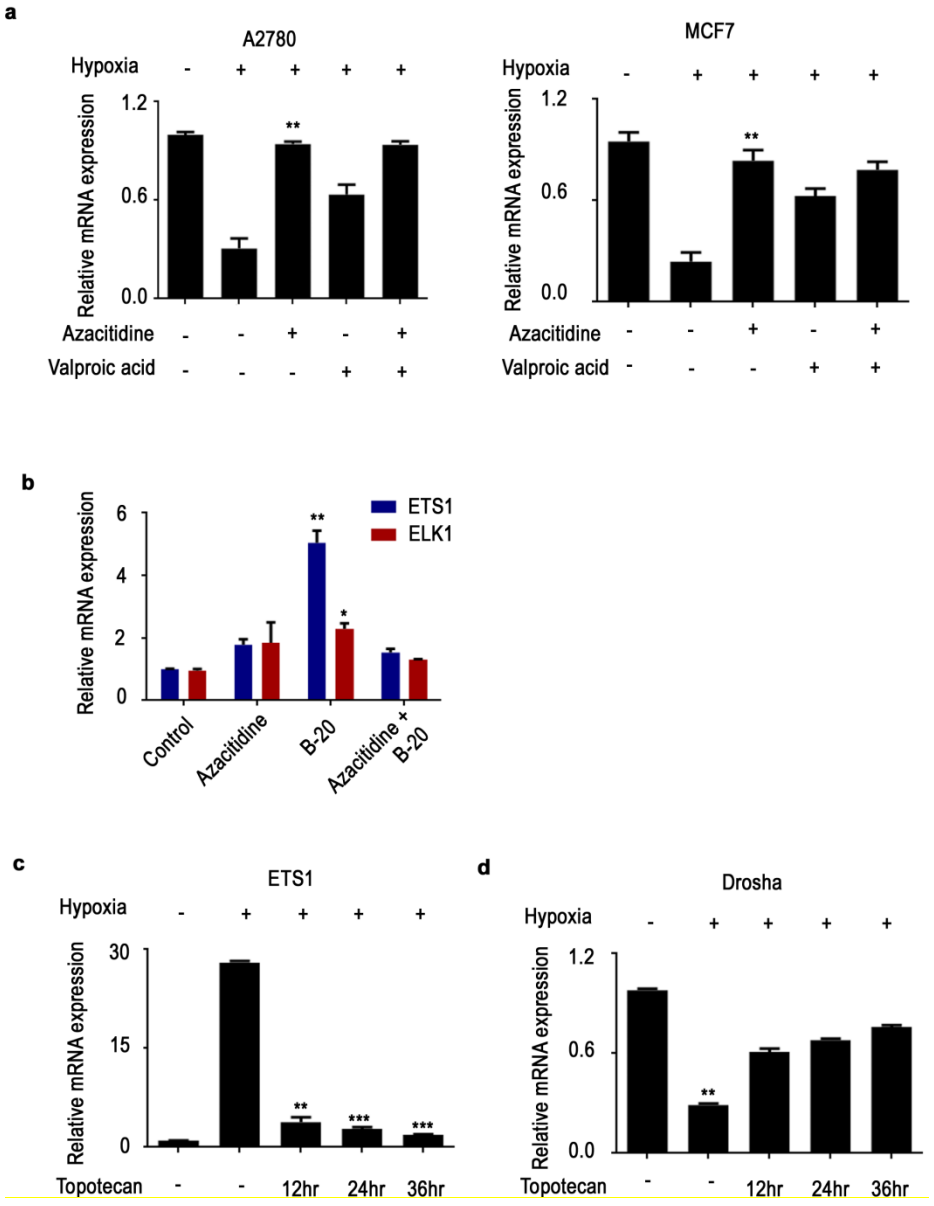

Supplementary Figure 10: (**a**) Drosha expression under hypoxic conditions in A2780 and MCF7 cells exposed to azacitidine and valproic acid either individually or in combination. (**b**) ETS1 and ELK1 expression levels in tumor samples treated with B-20, azacitidine, or both in a A2780 mouse model of ovarian cancer. ETS1 (**c**) and Drosha (**d**) expression in MCF7 cells treated with the HIF1α inhibitor topotecan under hypoxic conditions. Data are presented as mean ± standard error of the mean of n ≥ 3 independent experimental groups. *p < 0.05, **p < 0.01, ***p < 0.001 (Student *t* test).

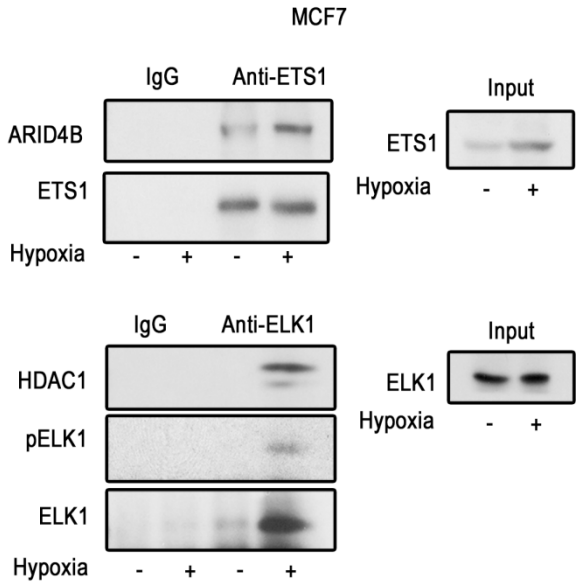

Supplementary Figure 11: Immunoprecipitation Western blots showing binding of ETS1 with ARID4B and binding of ELK1 with HDAC1 under hypoxic conditions in MCF7 cells. Data shown from a representative Western blot.

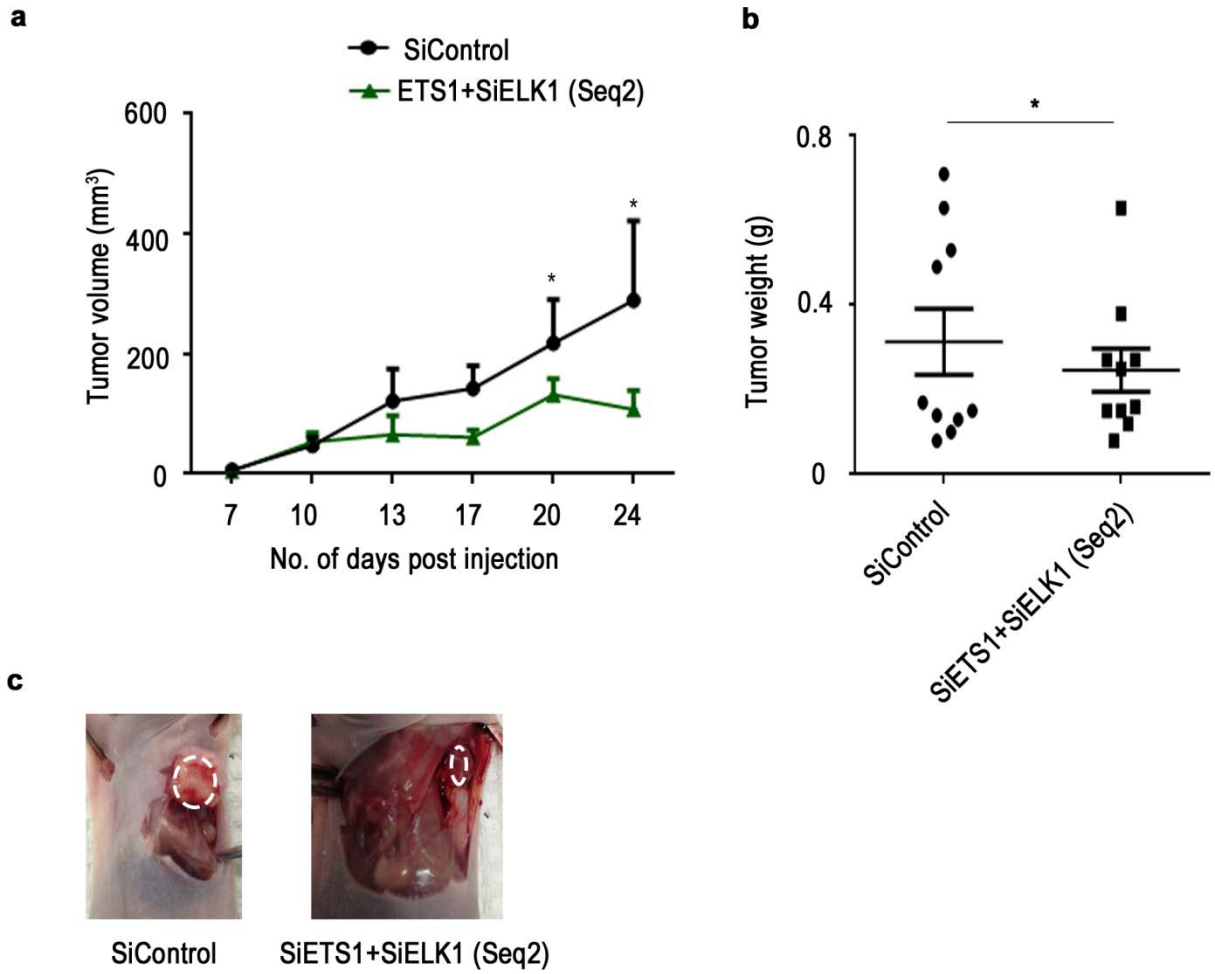

Supplementary Figure 12: Effect of silencing ETS1 and ELK1 using siRNAs (Seq2) in the MCF7 mouse model of breast cancer. Tumor volume (**a**) and aggregate tumor weight (**b**) across 2 groups. (**c**) Representative pictures showing tumor burden (white dotted circles) in all the groups. *p < 0.05 (Student *t* test).

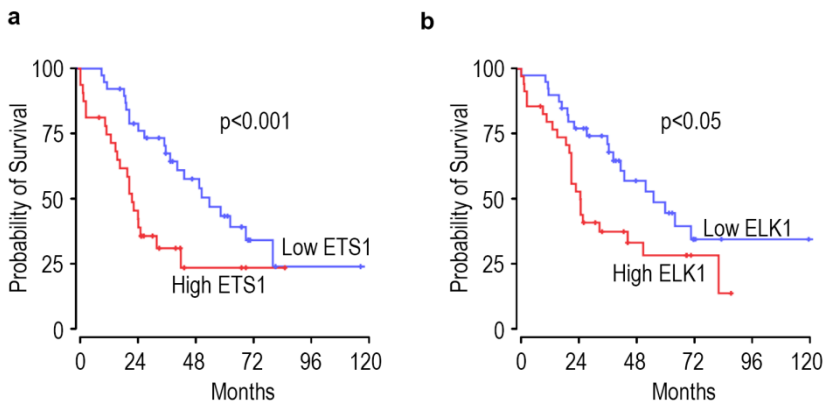

Supplementary Figure 13: Overall disease specific survival of patients with human high grade serous ovarian cancer (n=74) based on tumoral ETS1 (**a**) and ELK1 (**b**) mRNA expression levels. Kaplan-Meier curves shown; differences in survival were calculated using log rank method.

a

mRNA data (Normoxia vs Hypoxia)

Molecular function	p Value
Cellular Development	3.91E-15 to 1.35E-04
Cellular Growth and Proliferation	3.94E-15 to 1.35E-04
Cell Death	1.39E-14 to 1.42E-04
Cellular Movement	1.78E-14 to 1.40E-04
Cell Cycle	7.21E-13 to1.35E-04

miRNA data (Normoxia vs Hypoxia)

Molecular function	p Value
Cellular Movement	1.37E-06 to 4.27E-02
Cellular Growth and Proliferation	3.76E-05 to 4.83E-02
Cell Cycle	5.08E-05 to 4.55E-02
Cell Death	6.21E-05 to 3.71E-02
Cellular Development	8.23E-05 to 4.83E-02

b

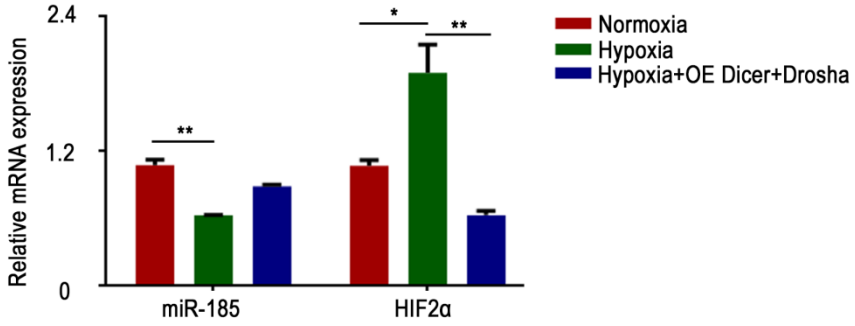

Supplementary Figure 14: (**a**) Top 5 molecular functions that are significantly altered as result of mRNAs (left) or miRNAs (right) deregulated under hypoxic condition. Data are from RNA deep sequencing and miRNA arrays from cells exposed to hypoxia and normoxia. Data were analyzed using ingenuity pathway network analysis. (**b**) Expression of miR-185 and HIF2α in A2780 cells exposed normoxia, hypoxia, and cells ectopically expressing Dicer and Drosha exposed hypoxia. Data are presented as mean ± standard error of the mean of n ≥ 3 independent experimental groups. *p<0.05, **p<0.01 (Student *t* test).

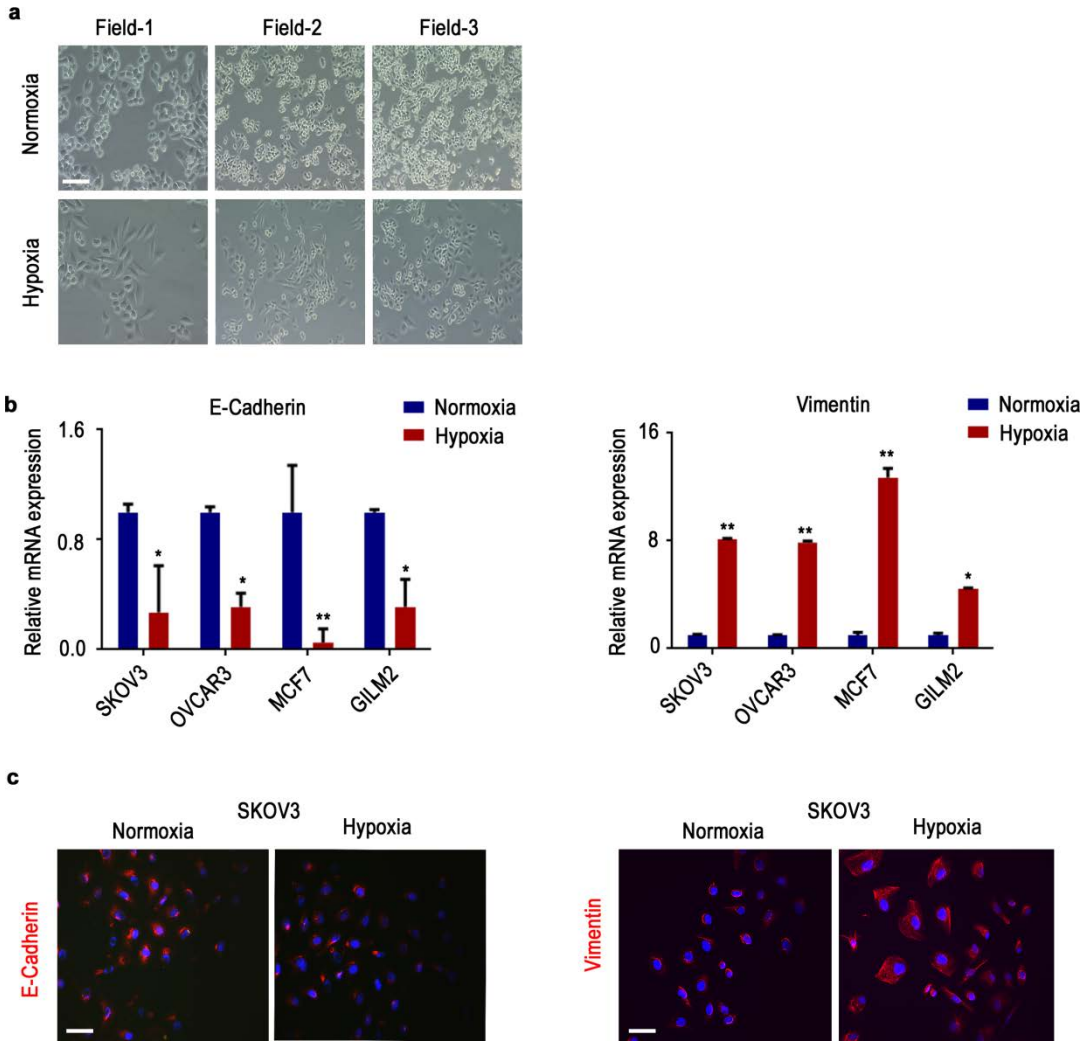

Supplementary Figure 15: (**a**) Phase contrast microscopy representative images showing cell morphology under normoxic and hypoxic conditions in A2780 cells. Scale bar: 400 µm. (**b**) E-cadherin (left) and vimentin (right) mRNA expression levels under hypoxic conditions in several types of cancer cells. (**c**) Protein levels of E-cadherin (left) and vimentin (right) under hypoxic conditions, assessed by immunofluorescent staining (red). Blue staining indicates the nucleus. Scale bar: 200 µm. Data are presented as mean ± standard error of the mean of n ≥_3 independent experimental groups. *p<0.05, **p < 0.01 (Student *t* test).

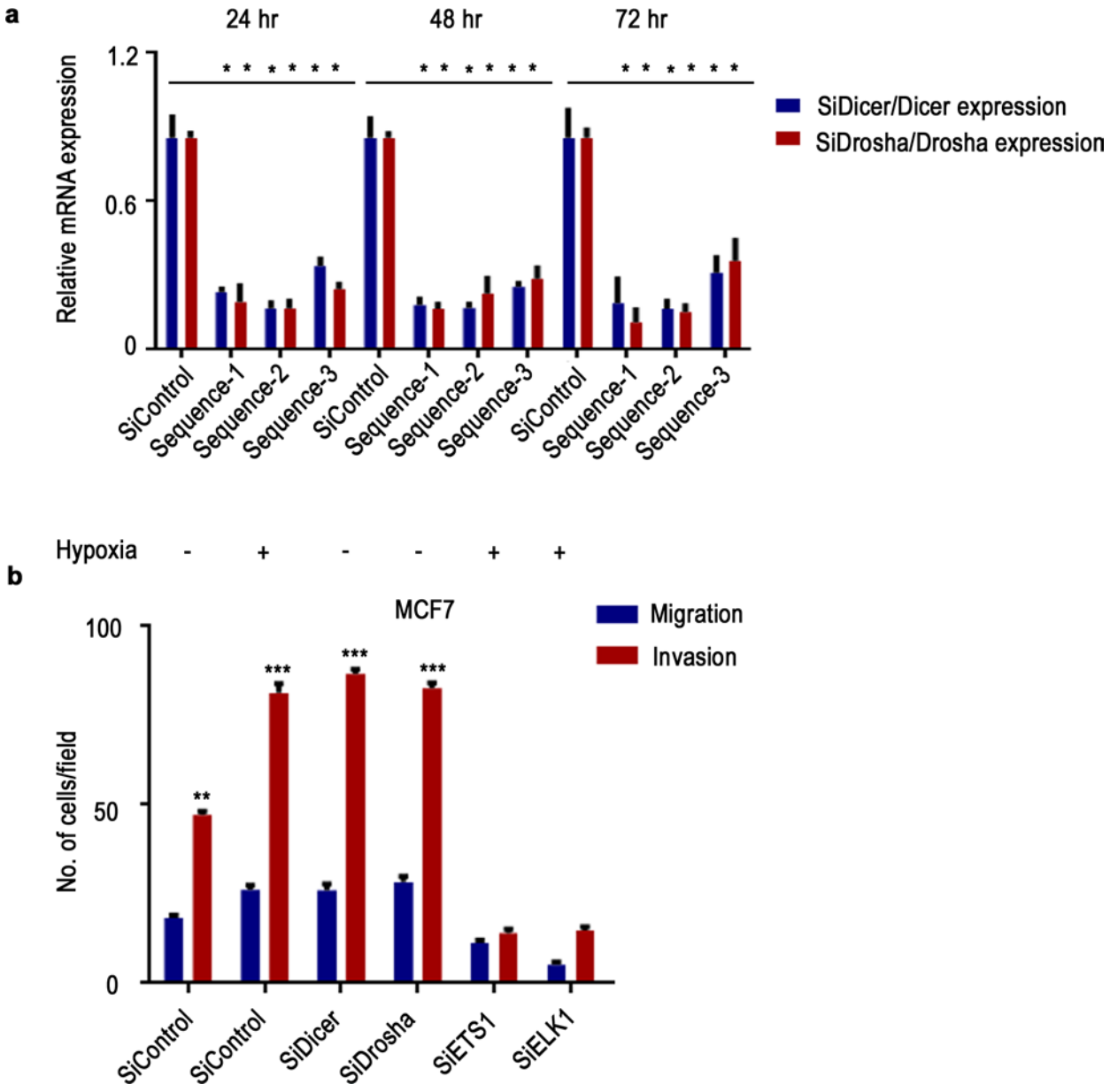

Supplementary Figure 16: (**a**) Drosha and Dicer relative mRNA expression levels after knockdown using 3 independent siRNA sequences across 3 different time points. (**b**) Migration and invasion of MCF7 cells after Drosha and Dicer knockdown (normoxia) and ETS1 and ELK1 knockdown (hypoxia). Data are presented as mean ± standard error of the mean of n ≥ 3 independent experimental groups. *p<0.05, **p < 0.01, ***p<0.001 (Student *t* test).

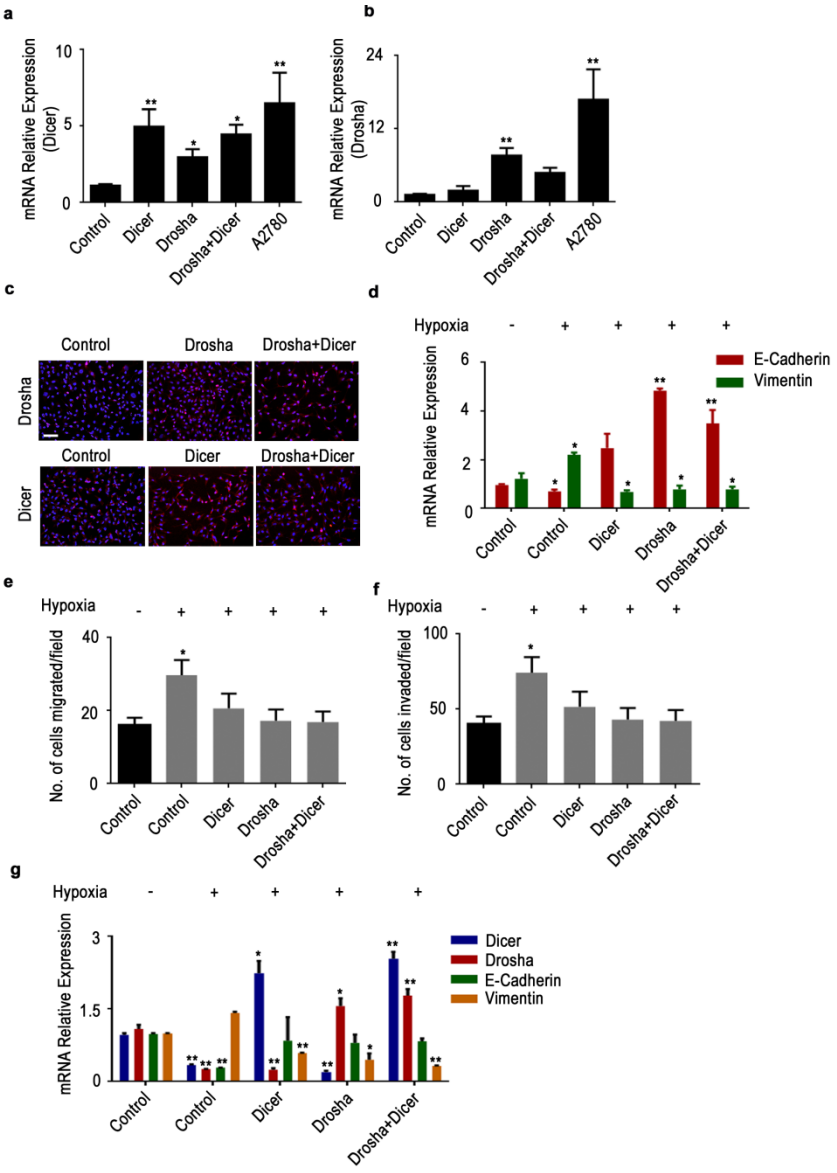

Supplementary Figure 17: **(a** and **b**) Dicer and Drosha mRNA expression levels in HeyA8 cell line variants ectopically expressing Dicer, Drosha, Drosha+Dicer, compared to relative levels in A2780 cells. (**c**) Protein levels of Drosha and Dicer in HeyA8 cells ectopically expressing Drosha, Dicer or both, analyzed using immunofluorescence microscopy. Scale bar: 200 µm. (**d**) Expression of E-Cadherin and Vimentin in the HeyA8 cells expressing Dicer, Drosha, or both and treated with hypoxia. Data were normalized to normoxic cells. (**e** and **f**) Migration and invasion assay data showing number of cells migrated or invaded in the respective groups of cells ectopically expressing Drosha, Dicer, or both and exposed to

hypoxia. (**g**) Expression of Dicer, Drosha, and EMT markers in A2780 cells exposed normoxia and hypoxia or in cells exposed to hypoxia while ectopically expressing Dicer, Drosha and Drosha+Dicer. Data are presented as mean ± standard error of the mean of n ≥ 3 independent experimental groups. *p<0.05, **p < 0.01 (Student *t* test).

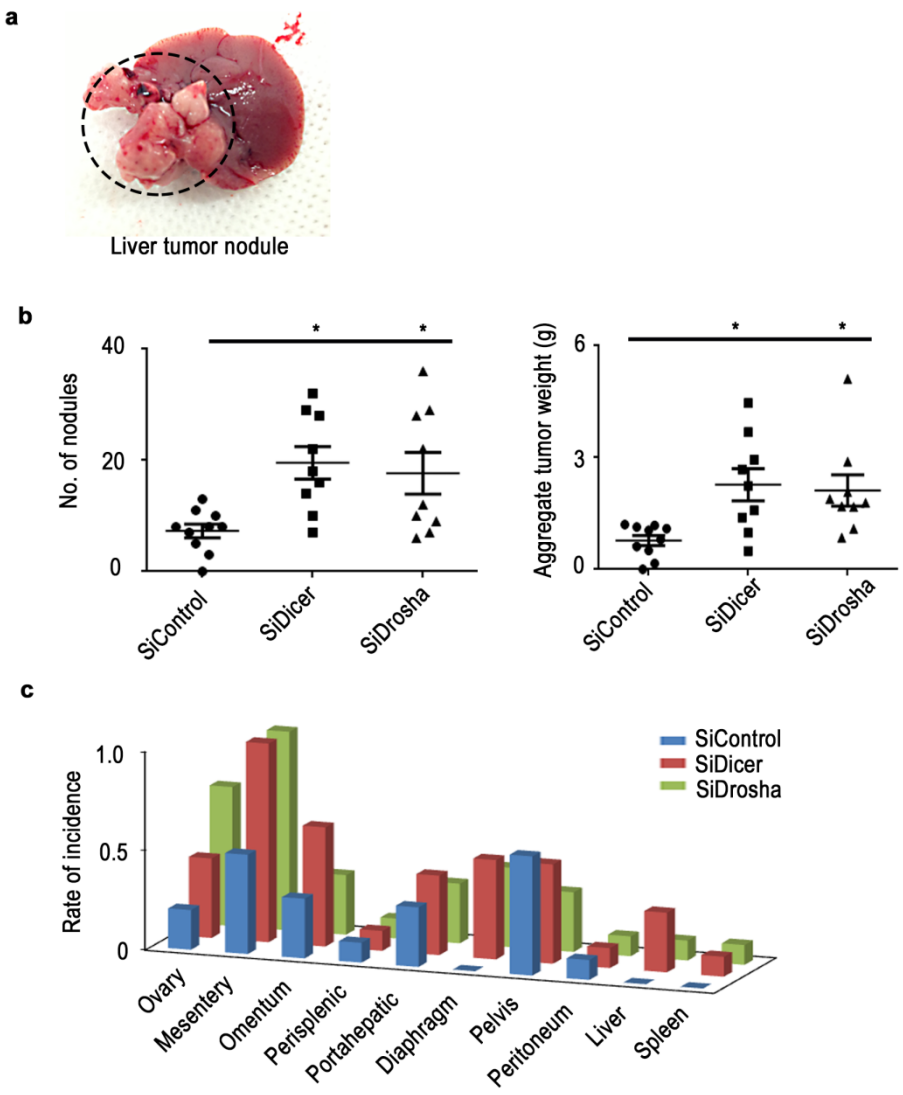

Supplementary Figure 18: (**a**) Photograph illustrating a rare liver metastatic nodule in A2780 orthotopic mice model group treated with siDicer and Drosha. (**b**) Average number of nodules and aggregate tumor weight in a late-stage metastasis model of ovarian cancer with Drosha and Dicer gene knockdown using siRNAs. (**c**) Tumor nodule rate of incidence in various metastatic sites in a late-stage metastasis model of ovarian cancer (A2780 cells) with Drosha and Dicer gene knockdown. n = 10 per group. *p<0.05 (Student *t* test).

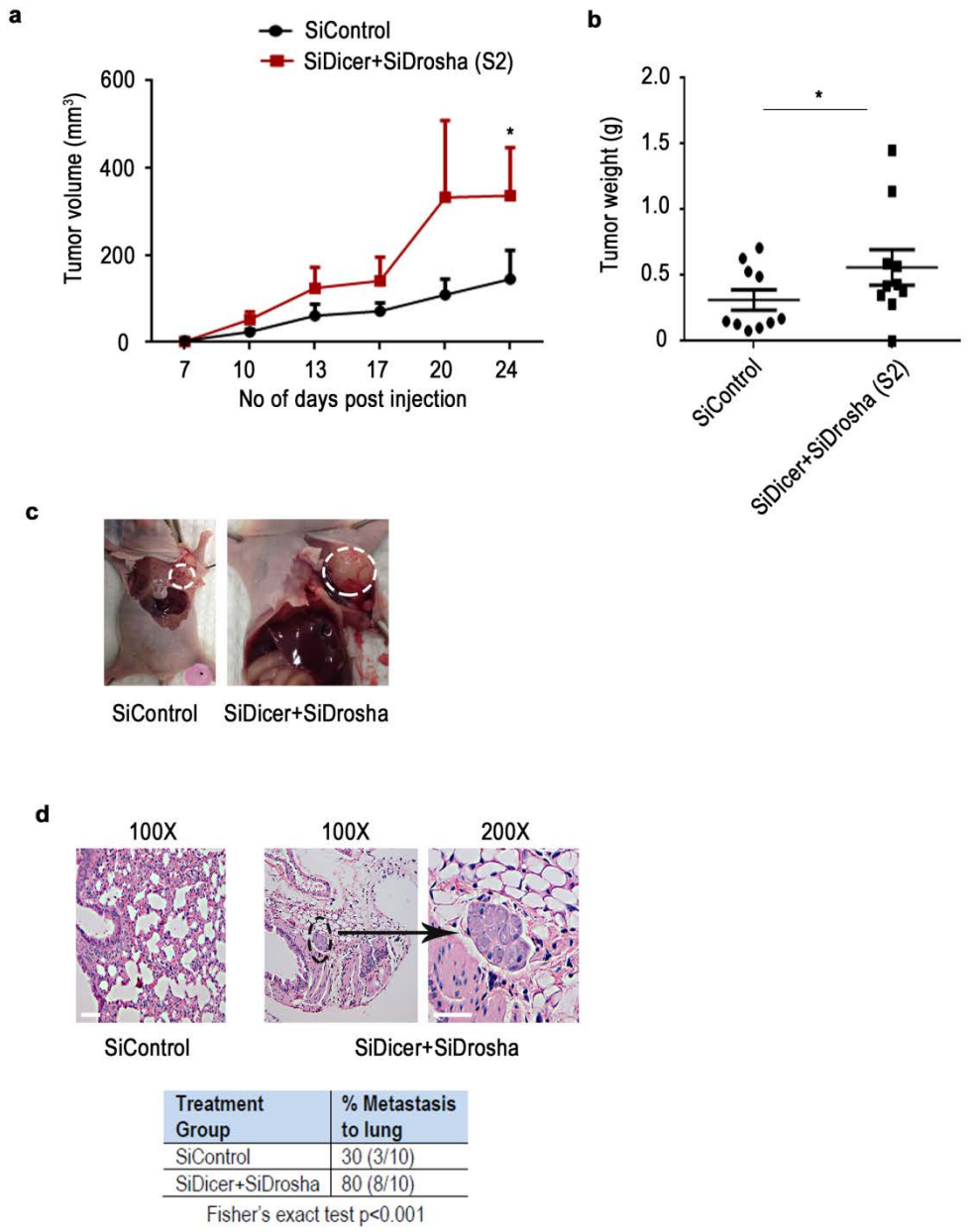

Treatment Group	% Metastasis to lung
SiControl	30 (3/10)
SiDicer+SiDrosha	80 (8/10)

Fisher's exact test p<0.001

Supplementary Figure 19: Effect of silencing Dicer and Drosha using siRNAs (seq 2) in the MCF7 mouse model of breast cancer. Tumor volume (**a**) and aggregate tumor weight (**b**) across 2 groups. (**c**) Representative pictures showing tumor burden (white dotted circles) in all the groups. *p < 0.05 (Student *t* test). (**d**) Representative hematoxylin and eosin staining of lungs from the *in vivo* MCF7 mouse model depicting micrometastases in the siDicer+Drosha group (top) and quantification of the micrometastases in the control and siDicer+siDrosha groups (bottom; n = 10 per group). Scale bar: 200 µm.

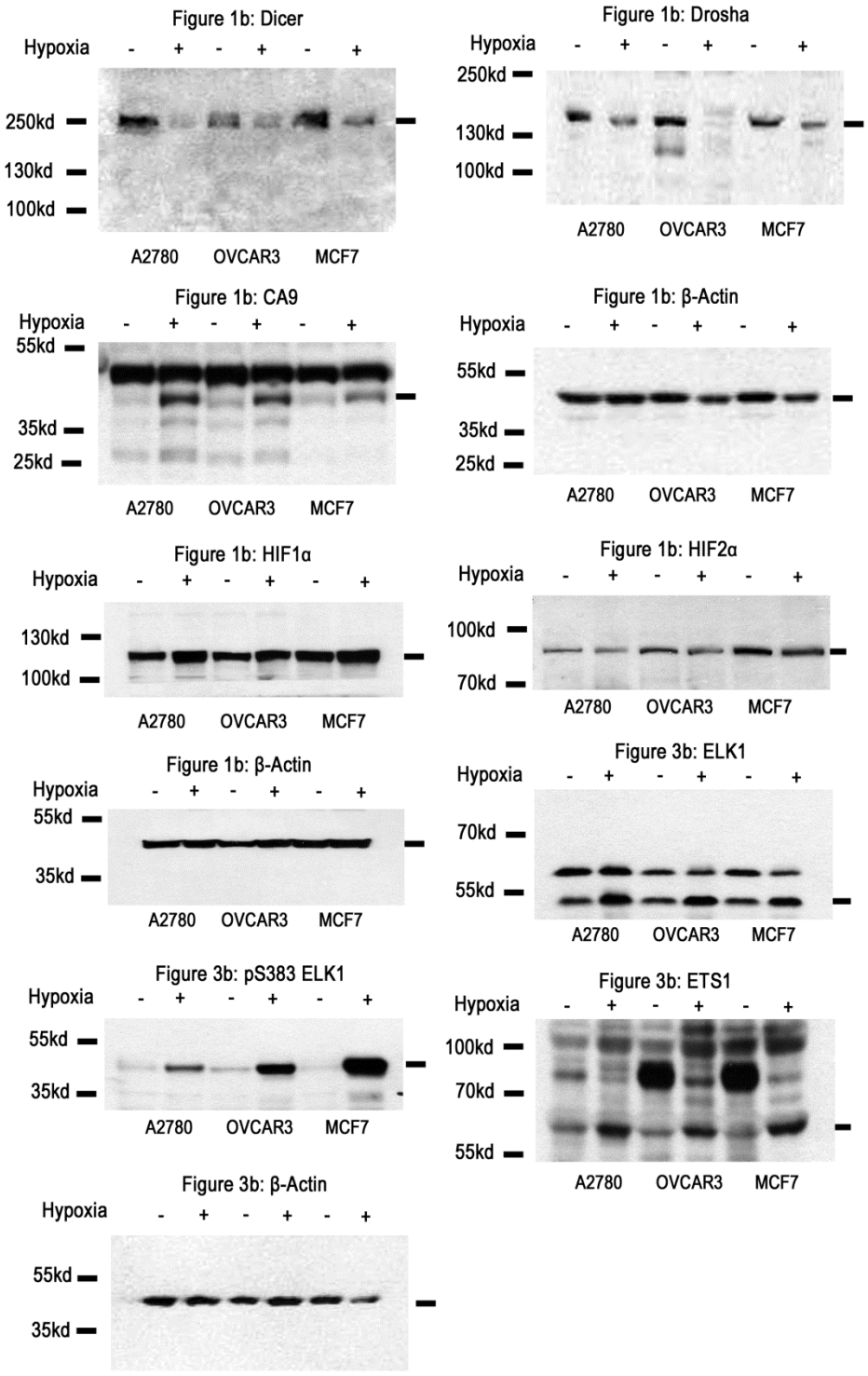

Supplementary Figure 20: Full scans of Western blots.

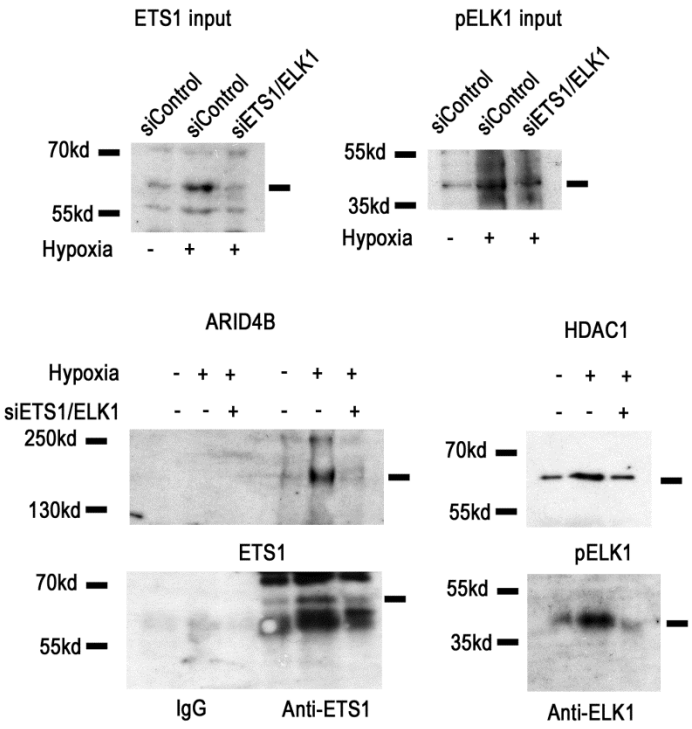

Supplementary Figure 21: Full scans of Western blots.

Supplementary Table 1: Primer and siRNA sequences used in the study.

Type	Gene	Sequence
SiRNA	Dicer Sequence 1	S 5’ CAUUGAUCCUGUCAUGGAU [dT] [dT] 3’
		AS 5’ AUCCAUGACAGGAUCAAUG [dT] [dT] 3’
	Dicer Sequence 2	S 5’ GCAGUUAUGAUUUAGCUAA [dT] [dT] 3’
		AS 5’ UUAGCUAAAUCAUAACUGC [dT] [dT] 3’
	Drosha Sequence 1	S 5’ CAGUAACUGUGACUGUUGU [dT] [dT] 3’
		AS 5’ ACAACAGUCACAGUUACUG [dT] [dT] 3’
	Drosha Sequence 2	S 5’ GGAUUAGCAACCUAUCCGA [dT] [dT] 3’
		AS 5’ UCCGAUAGGUUGCUAAUCC [dT] [dT] 3’
	ETS1 Sequence 1	S 5’ GUGAAACCAUAUCAAGUUA [dT] [dT] 3’
		AS 5’ UAACUUGAUAUGGUUUCAC [dT] [dT] 3’
	ETS1 Sequence 2	S 5’ CAUAUCAAGUUAAUGGAGU [dT] [dT] 3’
		AS 5’ ACUCCAUUAACUUGAUAUG [dT] [dT] 3’
	ELK1 Sequence 1	S 5’ GGGUUUGUGUGCCAGAAACCA [dT] [dT] 3’
		AS 5’ UGGUUUCUGGCACAAACCC [dT] [dT] 3’
	ELK1 Sequence 2	S 5’ CCUUACACGUCUCCUACUU [dT] [dT] 3’
		AS 5’ AAGUAGGAGACGUGUAAGG [dT] [dT] 3’
	HIF1α Sequence	S 5’ CUGAUGACCAGCAACUUGA [dT] [dT] 3’
		AS 5’ UCAAGUUGCUGGUCAUCAG [dT] [dT] 3’
Primers	ETS1	F 5’TGGGGACATCTTATGGGAAC3’ R 5’ATTCTGGATAGGCTGGGTTG3’
	ELK1	F 5’GGCCTTGCGGTACTACTATGAC3’ R 5’CCTCAGGGTAGGACACAAAC3’
	E Cadherin	F 5’GACCGGTGCAATCTTCAAA3’ R 5’TTGACGCCGAGAGCTACAC3’
	Vimentin	F 5’ATTCCACTTTGCGTTCAAGG3’ R 5’CTTCAGAGAGAGGAAGCCGA3’
	CA9	F 5’CAGCAACTGCTCATAGGCAC3’ R 5’CTTTGCCAGAGTTGACGAGG3’
	GLUT1	F 5’GGCATTGATGACTCCAGTGTT3’ R 5’ATGGAGCCCAGCAGCAA3’
	Drosha UM	F 5’GTTTTAAAGGGTTTTTTGTTGATGA3’ R 5’AAAACAAAACCAAACTACTACCACA 3’
	Drosha M	F 5’GGTTTTAAAGGGTTTTTTGTTGAC3’ R 5’CAAAACAAAACCAAACTACTACCG3’
	Drosha (qMethyl Light)	F 5’ ACGTAGGGGGAGGGGGCGCG3’ R 5’ACCGCCCGCGCCTCCGGAACA3’
	Drosha ChIP	F 5’ATTCCCTCGGTTTCCTGTTC3’ R 5’TCAGAGCAAAGCCAGGCTAC 3’
	Drosha ChIP -ve control	F 5’GAGCCTTAAATGCCAAGCAC3’ R 5’ACTGCGCCTGACTCCTTATTAC 3’
	Drosha promoter ETS1 mut	F 5’AATTCCCTCGGTTTCCTGTTAAAAAGGCGCGGGCGGTGCCACTGTCTTG 3’ R 5’CAAGACAGTGGCACCGCCCGCGCCTTTTTAACAGGAAACCGAGGGAATT3’
	Drosha promoter ELK1 mut	F 5’GGTTTGCTTTTTAATTCCCTCGGTAAAATGAAAAGGAGGCGCGGGCGGTG3’ R 5’CACCGCCCGCGCCTCCTTTTCATTTTACCGAGGGAATTAAAAAGCAAACC3’
	18s	F 5’CGCCGCTAGAGGTGAAATTC3’ R 5’TTGGCAAATGCTTTCGCTC3’
	STAT1	F 5’TGAATATTCCCCGACTGAGC3’ R 5’AGGAAGACCCAATCCAGATGT3’
	RHOB1	F 5’GGGACAGAAGTGCTTCACCT3’ R 5’CGACGTCATTCTCATGTGCT3’
	TAGLN	F 5’CTCATGCCATAGGAAGGACC3’ R 5’GTCCGAACCCAGACACAAGT 3’
	SERTAD2	F 5’AGCCCATCTTCATGCTCATC3’ R 5’CCTCCTGATGCGTTAGTTCC 3’
	TXNIP	F 5’AGGAAGCTCAAAGCCGAACT3’ R 5’ACGCTTCTTCTGGAAGACCA3’
	JAG1	F 5’ACTGTCAGGTTGAACGGTGTC3’ R 5’ATCGTGCTGCCTTTCAGTTT3’
	JUN	F 5’TCTCACAAACCTCCCTCCTG3’ R 5’GAGGGGGTTACAAACTGCAA3’
	CTGF	F 5’TGGAGATTTTGGGAGTACGG3’ R 5’CAGGCTAGAGAAGCAGAGCC3’
	HIF2a	F 5’ CATCCCGGGACTTCTCCT 3' R 5' GTCTGAACGTCTCAAAGGGC 3'□
	VEGF	F 5’ AGCTGCGCTGATAGACATCC□3' R 5' CTACCTCCACCATGCCAAGT□3'□

Matinspector analysis output file showing potential transcription factors binding Drosha promoter region.

LOCUS GXP_1499389(RNASEN/human) 716 bp DNA
DEFINITION loc=GXL_159340|sym=RNASEN|geneid=29102|acc=GXP_1499389|
taxid=9606|spec=Homo sapiens|chr=5|ctg=NC_000005|str=(-)|
start=31532067|end=31532782|len=716|tss=501,567,613,615,616|
descr=ribonuclease type III, nuclear|
comm=GXT_22785376/AK308093/616/gold;
GXT_22794494/NM_013235/501/silver;
GXT_22794496/NM_001100412/501/silver;
GXT_23730500/ENST00000511367/615/gold;
GXT_23730501/ENST00000504483/613/gold;
GXT_23730502/ENST00000513349/567/silver
ACCESSION GXP_1499389
COMMENT Matrix matches determined by MatInspector (Genomatix)
Matrix Family Library Version 8.3 (October 2010)
FEATURES Location/Qualifiers
misc_signal complement(5..19)
/note="V$NFKB/CREL.01, mat_sim: 0.920"
misc_signal complement(7..21)
/note="V$ZF5F/ZF5.01, mat_sim: 0.951"
misc_signal 11..27
/note="V$ABDB/HOXA9.02, mat_sim: 0.869"
misc_signal complement(11..29)
/note="V$CDXF/CDX2.02, mat_sim: 0.871"
misc_signal complement(17..27)
/note="V$RUSH/SMARCA3.01, mat_sim: 0.966"
misc_signal 16..32
/note="V$TALE/TGIF.01, mat_sim: 1.000"
misc_signal 23..33
/note="O$INRE/DINR.01, mat_sim: 0.974"
misc_signal complement(20..44)
/note="V$SORY/HBP1.01, mat_sim: 0.901"
misc_signal 30..42
/note="V$TEAF/TEAD.01, mat_sim: 0.902"
misc_signal 33..49
/note="V$ATBF/ATBF1.01, mat_sim: 0.820"
misc_signal 35..51
/note="V$BCL6/BCL6.01, mat_sim: 0.785"
misc_signal 36..52
/note="V$HNF1/HMBOX.01, mat_sim: 0.938"
misc_signal complement(45..59)
/note="V$RREB/RREB1.01, mat_sim: 0.830"
misc_signal 58..72
/note="V$DICE/DICE.01, mat_sim: 0.975"
misc_signal 60..78
/note="V$XBBF/RFXDC2.01, mat_sim: 0.908"
misc_signal 69..83
/note="V$MYBL/CMYB.02, mat_sim: 0.969"

misc_signal complement(79..93)
/note="V$MYBL/MYBL1.02, mat_sim: 0.841"
misc_signal 77..99
/note="V$PPAR/PPARG.01, mat_sim: 0.699"
misc_signal complement(82..100)
/note="V$HBOX/EN1.01, mat_sim: 0.784"
misc_signal complement(85..101)
/note="V$HNF1/HNF1.04, mat_sim: 0.846"
misc_signal complement(85..107)
/note="V$PAX2/PAX2.01, mat_sim: 0.857"
misc_signal 90..106
/note="V$HNF1/HMBOX.01, mat_sim: 0.937"
misc_signal complement(96..108)
/note="V$MYT1/MYT1L.01, mat_sim: 0.925"
misc_signal complement(95..111)
/note="V$HNF1/HNF1.04, mat_sim: 0.907"
misc_signal 115..135
/note="V$AP1R/MARE.02, mat_sim: 0.882"
misc_signal complement(123..149)
/note="V$CTCF/CTCF.03, mat_sim: 0.870"
misc_signal complement(132..146)
/note="V$CAAT/NFY.02, mat_sim: 0.838"
misc_signal complement(147..157)
/note="V$WHNF/WHN.01, mat_sim: 0.964"
misc_signal 151..161
/note="V$CSEN/DREAM.01, mat_sim: 0.970"
misc_signal complement(152..172)
/note="V$ETSF/SPI1_PU1.02, mat_sim: 0.968"
misc_signal complement(157..173)
/note="V$AP4R/AP4.01, mat_sim: 0.909"
misc_signal 161..181
/note="V$AP1R/MARE.02, mat_sim: 0.905"
misc_signal complement(195..219)
/note="V$RXRF/RAR_RXR.03, mat_sim: 0.826"
misc_signal 216..230
/note="V$GLIF/ZIC2.01, mat_sim: 0.914"
misc_signal complement(217..231)
/note="V$HAML/AML3.01, mat_sim: 0.875"
misc_signal complement(217..233)
/note="V$EGRF/NGFIC.01, mat_sim: 0.827"
misc_signal complement(228..242)
/note="V$RREB/RREB1.01, mat_sim: 0.842"
misc_signal 233..249
/note="V$PARF/HLF.01, mat_sim: 0.843"
misc_signal 237..257
/note="V$CREB/TAXCREB.01, mat_sim: 0.849"
misc_signal 240..254
/note="V$MYBL/VMYB.04, mat_sim: 0.873"
misc_signal complement(250..268)
/note="V$GREF/ARE.01, mat_sim: 0.800"
misc_signal complement(252..268)

/note="V$E2FF/E2F3.01, mat_sim: 0.981"
misc_signal complement(253..267)
/note="V$ZF5F/ZF5.01, mat_sim: 0.960"
misc_signal 253..269
/note="V$E2FF/E2F2.01, mat_sim: 0.890"
misc_signal 254..268
/note="V$ZF5F/ZF5.02, mat_sim: 0.886"
misc_signal complement(259..275)
/note="V$EGRF/CKROX.01, mat_sim: 0.981"
misc_signal complement(255..281)
/note="V$CTCF/CTCF.04, mat_sim: 0.794"
misc_signal complement(270..286)
/note="V$PBXC/PBX1_MEIS1.01, mat_sim: 0.751"
misc_signal complement(273..285)
/note="V$AP1F/AP1.02, mat_sim: 0.878"
misc_signal 272..290
/note="V$PAX3/PAX3.02, mat_sim: 0.867"
misc_signal 277..291
/note="V$PAX8/PAX8.01, mat_sim: 0.919"
misc_signal complement(282..298)
/note="V$E2FF/E2F.02, mat_sim: 0.957"
misc_signal 286..300
/note="V$MTF1/MTF-1.02, mat_sim: 0.860"
misc_signal complement(292..306)
/note="V$MYBL/MYBL1.02, mat_sim: 0.836"
misc_signal 314..330
/note="V$MYOD/MYOD.01, mat_sim: 1.000"
misc_signal complement(315..331)
/note="V$MYOD/MYOGENIN.02, mat_sim: 0.918"
misc_signal complement(317..329)
/note="V$NEUR/ASCL2.01, mat_sim: 0.961"
misc_signal 329..345
/note="V$E2FF/E2F4_DP2.01, mat_sim: 0.843"
misc_signal 332..344
/note="V$IKRS/IK1.01, mat_sim: 0.924"
misc_signal 341..357
/note="V$E2FF/E2F3.02, mat_sim: 0.874"
misc_signal complement(341..367)
/note="V$CTCF/CTCF.04, mat_sim: 0.799"
misc_signal complement(346..362)
/note="V$EVI1/MEL1.02, mat_sim: 0.994"
misc_signal complement(349..361)
/note="V$DMTF/DMP1.01, mat_sim: 0.836"
misc_signal 358..376
/note="V$CP2F/TCFCP2L1.01, mat_sim: 0.889"
misc_signal 366..382
/note="V$KLFS/KLF7.02, mat_sim: 0.890"
misc_signal 367..383
/note="V$SP1F/SP1.02, mat_sim: 0.855"
misc_signal 372..382
/note="O$XCPE/XCPE1.01, mat_sim: 0.906"

misc_signal 368..388
/note="V$ETSF/SPI1_PU1.02, mat_sim: 0.964"
misc_signal complement(370..386)
/note="V$NRF1/NRF1.01, mat_sim: 0.790"
misc_signal 371..387
/note="V$NRF1/NRF1.01, mat_sim: 0.811"
misc_signal complement(375..389)
/note="V$ZF5F/ZF5.01, mat_sim: 0.951"
misc_signal complement(381..391)
/note="O$XCPE/XCPE1.01, mat_sim: 0.825"
misc_signal 380..394
/note="V$GCMF/GCM1.01, mat_sim: 0.866"
misc_signal 388..400
/note="V$GRHL/GRHL1.01, mat_sim: 0.914"
misc_signal complement(389..409)
/note="V$IRFF/IRF3.01, mat_sim: 0.879"
misc_signal complement(402..416)
/note="V$CAAT/NFY.04, mat_sim: 0.933"
misc_signal complement(410..426)
/note="V$HIFF/HIF1.01, mat_sim: 0.877"
misc_signal 408..434
/note="V$CTCF/CTCF.01, mat_sim: 0.818"
misc_signal complement(415..429)
/note="V$GCMF/GCM1.03, mat_sim: 0.861"
misc_signal 415..431
/note="V$KLFS/KLF6.01, mat_sim: 0.937"
misc_signal complement(413..435)
/note="V$ZF02/ZNF219.01, mat_sim: 0.913"
misc_signal 417..433
/note="V$EGRF/CKROX.01, mat_sim: 0.996"
misc_signal complement(418..432)
/note="V$ZF07/ZNF263.01, mat_sim: 0.982"
misc_signal 418..434
/note="V$SP1F/GC.01, mat_sim: 0.921"
misc_signal 419..435
/note="V$EGRF/WT1.01, mat_sim: 0.941"
misc_signal 421..433
/note="V$MAZF/MAZR.01, mat_sim: 0.916"
misc_signal complement(416..438)
/note="V$ZF02/ZBP89.01, mat_sim: 0.985"
misc_signal 421..437
/note="V$EGRF/EGR1.02, mat_sim: 0.959"
misc_signal 421..437
/note="V$KLFS/KLF6.01, mat_sim: 0.932"
misc_signal 419..441
/note="V$PLAG/PLAG1.02, mat_sim: 1.000"
misc_signal complement(419..441)
/note="V$ZF02/ZNF219.01, mat_sim: 0.989"
misc_signal 423..439
/note="V$KLFS/KKLF.01, mat_sim: 0.919"
misc_signal 424..440

/note="V$SP1F/SP4.01, mat_sim: 0.945"
misc_signal 425..439
/note="V$ZF5F/ZF5.01, mat_sim: 0.958"
misc_signal complement(430..436)
/note="O$TF2B/BRE.01, mat_sim: 1.000"
misc_signal complement(422..444)
/note="V$ZF02/ZBP89.01, mat_sim: 0.934"
misc_signal complement(426..440)
/note="V$ZF5F/ZF5.02, mat_sim: 0.864"
misc_signal 428..440
/note="V$CDEF/CDE.01, mat_sim: 0.901"
misc_signal 426..442
/note="V$E2FF/E2F.03, mat_sim: 0.857"
misc_signal 427..441
/note="V$ZF5F/ZF5.02, mat_sim: 0.845"
misc_signal 428..444
/note="V$NRF1/NRF1.01, mat_sim: 0.783"
misc_signal 425..447
/note="V$PLAG/PLAG1.02, mat_sim: 1.000"
misc_signal complement(425..447)
/note="V$ZF02/ZF9.01, mat_sim: 0.938"
misc_signal 429..443
/note="V$ZF5F/ZF5.02, mat_sim: 0.842"
misc_signal 432..448
/note="V$E2FF/E2F.02, mat_sim: 0.849"
misc_signal 434..450
/note="V$LEFF/LEF1.01, mat_sim: 0.875"
misc_signal 435..451
/note="V$OAZF/ROAZ.01, mat_sim: 0.758"
misc_signal 434..462
/note="V$PRDM/PRDM5.01, mat_sim: 0.730"
misc_signal 446..466
/note="V$AP1R/MARE.01, mat_sim: 0.997"
misc_signal 447..467
/note="V$CREB/CREB.02, mat_sim: 0.923"
misc_signal 440..478
/note="O$TF2D/INR_DPE.01, mat_sim: 0.723"
misc_signal complement(452..470)
/note="V$CLOX/CDP.02, mat_sim: 0.956"
misc_signal complement(455..469)
/note="V$CAAT/NFY.04, mat_sim: 0.932"
misc_signal 462..472
/note="V$SMAD/SMAD4.01, mat_sim: 0.993"
misc_signal complement(465..475)
/note="V$SMAD/SMAD4.01, mat_sim: 0.993"
misc_signal 472..486
/note="V$HZIP/HOMEZ.01, mat_sim: 0.832"
misc_signal 479..499
/note="V$CREB/CREB.02, mat_sim: 0.944"
misc_signal complement(482..500)
/note="V$PAX6/PAX6.01, mat_sim: 0.751"

misc_signal complement(484..500)
/note="V$E2FF/E2F4_DP1.01, mat_sim: 0.964"
misc_signal 485..501
/note="V$E2FF/E2F4_DP1.01, mat_sim: 0.959"
misc_signal 485..503
/note="V$PAX6/PAX6.03, mat_sim: 0.835"
misc_signal 487..503
/note="V$E2FF/RB_E2F1_DP1.01, mat_sim: 0.739"
misc_signal complement(490..502)
/note="V$YBXF/YB1.01, mat_sim: 0.907"
misc_signal complement(489..505)
/note="V$PBXC/PBX1_MEIS1.01, mat_sim: 0.777"
misc_signal 491..505
/note="V$CAAT/NFY.04, mat_sim: 0.962"
misc_signal 490..508
/note="V$CLOX/CDP.02, mat_sim: 0.980"
misc_signal 494..508
/note="V$GFI1/GFI1.02, mat_sim: 0.909"
misc_signal complement(493..511)
/note="V$HOMF/TLX1.01, mat_sim: 0.960"
misc_signal complement(498..510)
/note="V$CDEF/CDE.01, mat_sim: 0.889"
misc_signal complement(499..513)
/note="V$ZF5F/ZF5.01, mat_sim: 0.953"
misc_signal complement(506..526)
/note="V$MOKF/MOK2.02, mat_sim: 0.997"
misc_signal complement(509..529)
/note="O$MTEN/DMTE.01, mat_sim: 0.804"
misc_signal 507..533
/note="V$CTCF/CTCF.03, mat_sim: 0.766"
misc_signal complement(518..532)
/note="V$SREB/SREBP.02, mat_sim: 0.838"
misc_signal complement(524..542)
/note="V$NFAT/NFAT5.02, mat_sim: 0.903"
misc_signal complement(531..547)
/note="V$E2FF/E2F.01, mat_sim: 0.782"
misc_signal complement(534..544)
/note="V$SPZ1/SPZ1.01, mat_sim: 0.946"
misc_signal complement(547..559)
/note="V$MYT1/MYT1L.01, mat_sim: 0.950"
misc_signal 556..568
/note="V$MEF3/SIX.01, mat_sim: 0.920"
misc_signal complement(561..581)
/note="V$ARID/BRIGHT.01, mat_sim: 0.936"
misc_signal 562..580
/note="V$HOMF/HHEX.01, mat_sim: 0.976"
misc_signal 564..580
/note="V$ATBF/ATBF1.01, mat_sim: 0.816"
misc_signal complement(563..581)
/note="V$BRNF/TST1.01, mat_sim: 0.983"
misc_signal complement(563..583)

/note="V$CART/ALX4.01, mat_sim: 0.821"
misc_signal 565..583
/note="V$CDXF/CDX1.02, mat_sim: 0.845"
misc_signal complement(565..583)
/note="V$HBOX/EN1.01, mat_sim: 0.782"
misc_signal complement(565..583)
/note="V$HOXF/HOXB8.01, mat_sim: 0.892"
misc_signal complement(567..583)
/note="V$ABDB/HOXC9.01, mat_sim: 0.863"
misc_signal 566..584
/note="V$HOMF/MSX.01, mat_sim: 0.977"
misc_signal 568..582
/note="V$NKX6/NKX61.01, mat_sim: 0.954"
misc_signal 568..586
/note="V$HOXF/HOXC8.01, mat_sim: 0.851"
misc_signal 579..591
/note="V$ZFHX/AREB6.04, mat_sim: 0.985"
misc_signal complement(577..597)
/note="V$ETSF/ELK1.02, mat_sim: 0.910"
misc_signal complement(578..598)
/note="V$IRFF/IRF7.01, mat_sim: 0.870"
misc_signal complement(583..603)
/note="V$ETSF/ELK1.02, mat_sim: 0.938"
misc_signal 588..608
/note="V$ETSF/CETS1P54.01, mat_sim: 0.921"
misc_signal complement(599..605)
/note="O$TF2B/BRE.01, mat_sim: 1.000"
misc_signal 595..611
/note="V$E2FF/E2F.03, mat_sim: 0.860"
misc_signal 596..612
/note="V$EGRF/EGR1.03, mat_sim: 0.902"
misc_signal complement(596..612)
/note="V$NRF1/NRF1.01, mat_sim: 0.792"
misc_signal 597..613
/note="V$NRF1/NRF1.01, mat_sim: 0.783"
misc_signal 591..621
/note="V$NRSF/NRSE.01, mat_sim: 0.698"
misc_signal 599..615
/note="V$SP1F/SP1.03, mat_sim: 0.928"
misc_signal 613..639
/note="V$AIRE/AIRE.01, mat_sim: 0.870"
misc_signal complement(639..655)
/note="V$LEFF/LEF1.03, mat_sim: 0.831"
misc_signal complement(643..661)
/note="V$SNAP/PSE.01, mat_sim: 0.859"
misc_signal 646..666
/note="V$CREB/ATF.01, mat_sim: 0.941"
misc_signal 664..684
/note="V$MOKF/MOK2.02, mat_sim: 0.994"
TATA binding misc_signal complement(672..688)
/note="O$VTBP/VTATA.01, mat_sim: 0.999"

misc_signal complement(675..689)
/note="O$PTBP/PTATA.02, mat_sim: 0.925"
misc_signal complement(675..691)
/note="V$ABDB/HOXD13.01, mat_sim: 0.941"
misc_signal 678..700
/note="V$PERO/PPARG.02, mat_sim: 0.895"
misc_signal 679..703
/note="V$NR2F/TR4.02, mat_sim: 0.787"
misc_signal 686..706
/note="V$MOKF/MOK2.02, mat_sim: 0.980"
misc_signal 684..708
/note="V$SORY/SOX9.03, mat_sim: 0.785"
misc_signal complement(685..709)
/note="V$SORY/SOX9.03, mat_sim: 0.811"
misc_signal 689..711
/note="V$PLAG/PLAGL1.02, mat_sim: 0.900"
misc_signal complement(693..707)
/note="V$SF1F/FTF.01, mat_sim: 0.970"
misc_signal complement(691..711)
/note="V$PTF1/PTF1.01, mat_sim: 0.761"
BASE COUNT 114 a 215 c 209 g 178 t

ORIGIN
ACTCGTAGGAAGCGCCCATAAATGTCAGTTCTCATTCTTCCTAGTTAGCTGTTTTGGGGTC
CTCTCCACAGCAACGGAATAGGGCAGTTTAACTCTGGTTAACTCTCTGGCCTCCGATGCTA
AGGTTGCGCCCTCTGCTTGGCCCTCTGAGCGTCAGGGCTTCCGCTGATTCTGCCCCAGAG
CCCTGTTGCCGTCCGCTCACCTCCTGATGATCCTCCACCACCCACACTGGGAGCTTGGGG
TAACGCCGGAGACCAGCGCGCCCTCCCGCGGAGTCACTCATGTTTTTGCGCCCGTCAGTT
TTGCAGTAAAGCGGTGGCAGCTGGAGAAGACCCGGGAAAGCCGGCGCCTCATCCCGGCC
AGCTCTCTCCGGGCGGAAGCGCTCCCTCACCCGGTTGCGTTTTCGGATTGGAGGACGTAG
GGGGAGGGGGCGCGGGCTCCAAAGGGTCTTTTGCTGACGATTGGTCTAGACGTCCATCG
CTTTCGTTGACGCGCCAATCACCGCGCACAAGGCCCTGCGGTGGGCTGAAGAGTTTTCCC
TCCCTTGGCCCAGCTTTCTCAGGTTTGCTTTTTAATTCCCTCGGTTTCCTGTTCCGGAGGC
GCGGGCGGTGCCACTGTCTTGGTACCTGCGGTAGTAGCCTGGCTTTGCTCTGACGGCGAT
CTCGCGGCCCGAGAGCCTTTTATAGGTAAAAGGGGTACCTTGCAAGTGTTAGAAG